

Please cite the Published Version

Heywood, Wendy E, Bliss, Emily, Bahelil, Fatima, Cyrus, Trinda, Crescente, Marilena , Jones, Timothy, Iqbal, Sadaf, Paredes, Laura G, Toner, Andrew J, del Arroyo, Ana G, O'Toole, Edel A, Mills, Kevin and Ackland, Gareth L (2021) Proteomic signatures for perioperative oxygen delivery in skin after major elective surgery: mechanistic sub-study of a randomised controlled trial. *British Journal of Anaesthesia*, 127 (4). pp. 511-520. ISSN 0007-0912

DOI: <https://doi.org/10.1016/j.bja.2021.06.003>

Publisher: Elsevier BV

Version: Accepted Version

Downloaded from: <https://e-space.mmu.ac.uk/628097/>

Usage rights:  [Creative Commons: Attribution-Noncommercial-No Derivative Works 4.0](https://creativecommons.org/licenses/by-nc-nd/4.0/)

Additional Information: This is an Accepted Manuscript of an article which appeared in *British Journal of Anaesthesia*, published by Elsevier

Enquiries:

If you have questions about this document, contact openresearch@mmu.ac.uk. Please include the URL of the record in e-space. If you believe that your, or a third party's rights have been compromised through this document please see our Take Down policy (available from <https://www.mmu.ac.uk/library/using-the-library/policies-and-guidelines>)

Proteomic signatures of perioperative oxygen delivery in skin after major elective surgery: mechanistic sub-study of a randomised controlled trial.

Wendy E. Heywood,¹ Emily Bliss,¹ Fatima Bahelil,¹ Trinda Cyrus,² Marilena Crescente,³ Timothy Jones,² Sadaf Iqbal,⁴ Laura Gallego Paredes,⁴ Andrew J. Toner,⁵ Ana Gutierrez del Arroyo,² Edel A. O'Toole,⁶ Kevin Mills,¹ Gareth L. Ackland²

1 Translational Mass Spectrometry Research Group, UCL Institute of Child Health, 30 Guilford Street, London, UK.

2 Translational Medicine & Therapeutics, William Harvey Research Institute, Queen Mary University of London, London, UK

3 Exeter University Medical School, UK.

4 Centre for Cell Biology and Cutaneous Research, Blizard Institute, Queen Mary University of London, London, UK

5 University College London NHS Hospitals Trust, London, UK.

6 Department of Anesthesia, Royal Perth Hospital, Perth, Western Australia, Australia.

7 Molecular Dermatology, Centre for Cell Biology and Cutaneous Research, Blizard Institute, Queen Mary University of London, London, UK

Correspondence to: G L Ackland, Professor of Perioperative Medicine, Translational Medicine & Therapeutics, William Harvey Research Institute, Queen Mary University of London, EC1M 6BQ. United Kingdom; g.ackland@qmul.ac.uk +44 20 3594 0351

Keywords: Surgery; randomized controlled trial; skin; proteomics; sepsis; wound infection.

Running title: Skin proteomics and perioperative morbidity.

Abstract

Background: Maintaining adequate oxygen delivery (DO_2) after major surgery is associated with minimizing organ dysfunction. Skin is particularly vulnerable to reduced oxygen delivery. We tested the hypothesis that reduced perioperative DO_2 fuels inflammation in metabolically compromised skin after major surgery.

Methods. Participants undergoing elective oesophagectomy were randomized immediately after surgery to standard of care or haemodynamic therapy to achieve their individualized preoperative DO_2 . Abdominal punch skin biopsies were snap-frozen before, and 48h after, surgery. On-line two-dimensional liquid chromatography and ultra-high definition label-free mass spectrometry characterised the skin proteome. The primary outcome was proteomic changes compared between normal (\Rightarrow preoperative value before induction of anaesthesia) and low DO_2 ($<$ preoperative value before induction of anaesthesia) after surgery. Secondary outcomes were functional enrichment analysis of up/down-regulated proteins (Ingenuity pathway analysis; STRING Protein-Protein Interaction Networks). Immunohistochemistry and immunoblotting confirmed selected proteomic findings in skin biopsies obtained from patients after hepatic resection.

Results. Paired punch skin biopsies were obtained from 35 participants (mean age:68y (9); 31% female), of whom 17 underwent oesophagectomy. 14/2096 proteins were associated with normal ($n=10$) versus low ($n=7$) DO_2 after oesophagectomy. Failure to maintain preoperative DO_2 was associated with upregulation of proteins counteracting oxidative stress. Normal DO_2 after surgery was associated with pathways involving leucocyte recruitment and upregulation of an antimicrobial peptidoglycan recognition protein. Immunohistochemistry ($n=6$ patients) and immunoblots after liver resection in patients ($n=12$) supported the proteomic findings.

Conclusions. Proteomic profiles in serial skin biopsies identify organ-protective mechanisms

associated with normal DO₂ following major surgery.

Trial registration. ISRCTN76894700

Funding. Academy of Medical Sciences/Health Foundation Clinician Scientist Award CSF3 [GLA]; British Oxygen Company research chair grant in Anesthesia [GLA]; Great Ormond Street Hospital Biomedical Research Centre [EB,WH,KM]; British Heart Foundation: PG/17/40/33028 [MC]; UK NIHR [GLA]; Barts Charity [TJ]

Introduction

Mass-spectrometry based proteomics provide novel information that is not discernable through genomic analyses alone.¹ Enzymatic digestion of proteins extracted from biological samples into peptides enables analysis by liquid chromatography–tandem mass spectrometry (LC-MS/MS). Briefly, LC-MS/MS quantifies proteins by the mass-to-charge ratio of ionised peptides, or fragments of peptides. Computational algorithms identify proteins by correlating known masses with the spectra of the signal intensity of detected ions as a function of the mass-to-charge ratio.² Other than a single study of plasma proteomics,³ no perioperative studies have thus far employed proteomics to examine serial changes at the end-organ level.

Complications after elective esophagectomy and major intra-abdominal surgery occur in ~20% of patients, resulting in delayed discharge and/or readmission to hospital.⁴ Avoiding even minor complications after major surgery appears to be pivotal in determining survival, extending until after hospital discharge.⁵ Maintaining oxygen delivery is strongly associated with minimising organ dysfunction and reducing morbidity after surgery.⁶⁻⁹ Although the mechanisms that trigger complications associated with the failure to preserve oxygen delivery remain unclear, the intersection between metabolic dysfunction and inflammation may be key.^{10, 11}

Skin is particularly vulnerable to reductions in cardiac output and hence oxygen delivery, as blood is preferentially shunted away from skin to preserve the perfusion of vital organs.¹² Direct injury to the skin triggers an immunometabolic response that coordinates wound healing.¹³ Even after distant injury, cytokine production is up-regulated in uninjured skin from a range of skin-resident cells.¹⁴ Skin-derived mediators contribute to systemic inflammation and organ dysfunction through lymph node drainage.¹⁵ The skin proteome may, therefore, reveal mechanistic insight into how organs are impacted by reduced oxygen delivery after major surgery.

Here, we tested the hypothesis that reduced oxygen delivery after major surgery fuels organ injury through inflammation generated by metabolically compromised skin. We used LC-MS/MS to serially quantify the skin proteome in patients enrolled in a randomised controlled trial which demonstrated that morbidity was less frequent in patients in whom preoperative oxygen delivery values was maintained after surgery (regardless of goal-directed haemodynamic therapy).⁸

Methods

Subjects

Adult patients undergoing major elective surgery who were enrolled in the Postoperative Morbidity Oxygen delivery (POM-O) study gave written informed consent for skin biopsy samples to be obtained. POM-O was a multicentre, double-blind, randomised controlled trial done in four university hospitals in the UK (ISRCTN76894700), approved by the South London Research Ethics Committee Office (09/H0805/58).⁶

Inclusion criteria

Surgery expected to last for at least 120 min were eligible for recruitment provided they satisfied the following high-risk criteria: American Society of Anesthesiologists classification of 3 or more; surgical procedures with an estimated or documented risk of postoperative morbidity (as defined by the Postoperative Morbidity Survey) exceeding 50%; modified Revised Cardiac Risk Score of 3 or more, as defined by age 70 years or more, a history of cardiovascular disease (myocardial infarction, coronary artery disease, cerebrovascular accident, electrocardiographic evidence for established cardiac pathology), cardiac failure, poor exercise capacity (anaerobic threshold <11 mL/kg per min assessed by cardiopulmonary exercise testing or Duke Activity Status Index), renal impairment (serum creatinine \geq 130 μ mol/L), or diabetes.

Exclusion criteria

Refusal of consent, pregnancy, lithium therapy or allergy, recent myocardial ischaemia (within the previous 30 days), acute arrhythmia, acute bleeding, and patients receiving palliative treatment only.

Intervention

Patients were allocated by computer-generated randomisation to a postoperative protocol (intravenous fluid, with and without dobutamine) targeted to achieve their individual preoperative oxygen delivery value (goal-directed therapy) or standardised care (control).

Patients and staff were masked to the intervention. The primary outcome of the original parent study was absolute risk reduction in morbidity (defined by Clavien-Dindo grade II or more)¹⁶ on postoperative day 2.

Skin biopsy and sample preparation

2mm skin punch biopsies (Instrapac, Robinson Healthcare, Worksop, UK) were obtained before surgery within 5cm of the surgical incision immediately after the induction of general anaesthesia (Figure 1). A repeat biopsy was obtained 48 hours after surgery on the opposite side of the surgical incision (under local anaesthesia). Punch biopsies were immediately snap frozen in liquid nitrogen or immersed in 4% paraformaldehyde. For proteomic analyses, samples were prepared as described previously.¹⁷ Snap-frozen samples were homogenised in 50mM ammonium bicarbonate and 2% w/v ASB-14 using bead (Precellys 1.4mm diameter ceramic beads, Peqlab, VWR) and mechanical homogenisation (Minilys®, Bertin Technologies). A modified Lowry protein assay (Pierce™, ThermoFisher Scientific) was used to calculate the protein content and 50 µg was lyophilised using a freeze drier. Proteins were resolubilised in 100 mmol L⁻¹ TRIS-HCL, pH 7.8, containing 2% w/v ASB-14, 6 mol L⁻¹ urea and 2 mol L⁻¹ thioiurea and digested using Sequencing Grade Modified Trypsin (Promega, Madison, USA).

Two-dimensional liquid chromatography.

Following in-solution digestion of the homogenised sample, purification of the digested sample peptides reverse phase C-18 chromatography was undertaken to remove the salt and lipid content of the sample (ISOLUTE® C18 columns, Biotage, Ystrad Mynach, UK), as described previously.¹⁷ Then, two dimensional high pH fractionation of sample peptides, followed by low pH chromatographic separation using an online nanoAcquity ultra high performance liquid chromatography system was undertaken (Supplementary data). For each fraction, a 60 min mass spectrometry analysis was performed on a SYNAPT G2-Si (Waters, Manchester, UK) mass spectrometer (Waters, Manchester, UK) in a UDMS^E positive ion electrospray ionisation mode.¹⁸

Proteomic analysis

Raw mass spectrometry data were processed using Progenesis QI analysis software (Nonlinear Dynamics, U.K.). Peptide identifications were performed using MS^e search identification against the Uniprot Human reference proteome 2015, with 1 missed cleavage and 1% peptide false discovery rate (FDR).¹⁹ Fixed modifications were set to carbamidomethylation of cysteines and dynamic modifications of hydroxylation of aspartic acid, lysine, asparagine and proline and oxidation of methionine. A protein was considered to be differentially expressed if there was a significant change ($p < 0.05$) from preoperative values accounting for the degree, direction, and rank of difference between samples obtained before and 48h after surgery with sequence length ≥ 6 , hits ≥ 2 , a maximal mean fold change ≥ 1.5 and >20 -confidence score, a further measure of false-discovery rate (Progenesis QI). Proteomics data was deposited in the PRIDE PRoteomics IDentifications (PRIDE) public-domain repository, which provides a single point for submitting mass spectrometry based

proteomics data.²⁰ Data was normalised and significance determined by one-way ANOVA analysis (Progenesis QI software).

Immunohistochemistry

Immunofluorescence on frozen sections of human skin biopsies was used to confirm selected findings from the proteomic data by histologists masked to clinical details (Atlantic Bone Screen, Cedex, France). Using validated antibodies (Supplementary data), protein expression of epidermal integrin alpha-6 (ITGA6; 1:50; Merck Millipore (MAB1378)) and the cell surface glycoprotein CD44 (1:50; Novocastra (BMS144)) were quantified by immunofluorescence by an investigator masked to clinical details (Fiji software, NIH Image, USA).

Immunoblots

Membranes were incubated with the following species-specific primary antibodies for parkin and superoxide dismutase-1 to confirm selected findings from the proteomic data, which were masked to clinical details. Secondary antibodies (1:2000) were rabbit anti-mouse HRP (Dako, Stockport, UK) or goat anti-rabbit HRP (Cell Signaling Technology, Leiden), as indicated. Membranes were developed using ECLTM reagent and Hyperfilm ECL (Amersham, UK).

Primary outcome

The primary outcome was differential protein expression (before versus after surgery), compared between individuals with DO₂ defined as normal (same or higher than each individual's preoperative value) or low (less than each individual's preoperative value).

Secondary outcomes- functional pathway analysis.

We assessed categorical changes in skin protein expression (as defined by fold-change and confidence scores) before and after surgery using the STRING database, which collects, scores and integrates all publicly available sources of protein-protein interaction information through which computational predictions for direct (physical) as well as indirect (functional) interactions are made.²¹ For the enrichment analysis, STRING employs the established classification systems Gene Ontology²² and KEGG²³ but also offers additional, new classification systems based on high-throughput text-mining as well as on a hierarchical clustering of the association network itself. To compare quantitative fold-changes in protein expression between oxygen delivery achievers versus non-achievers, we used Ingenuity Pathways Analysis (IPA) (01-13) software (Qiagen, USA) to perform enrichment analyses²⁴ to estimate the significance of observing a candidate protein set within the context of biological systems.²⁵ Protein identifiers were mapped in the Ingenuity Pathway Knowledge Base to find cellular functions and diseases significantly associated with differentially expressed proteins. We determined changes in biological processes associated with differential protein expression by using downstream effect analysis. Molecular interactions between proteins and affected functions were visualised using network analysis.

Statistical analyses

All analyses were conducted by investigators blinded to the identity of treatments/genotypes. Clinical data were processed by analysers blinded to patient group assignments. For all statistical tests, the Benjamin-Hochberg procedure was applied where applicable to correct for testing multiple hypotheses. Data distribution was assessed by the Kolmogorov-Smirnov normality test. P values < 0.05 were considered significant.

Sample size estimation

We estimated that 20 paired samples would achieve a power of 80% ($\alpha=0.05$) to detect an effect size of 0.7 between pairs where protein expression changed by ≥ 1.5 -fold (confidence score > 20).

Results

Participant characteristics.

Paired punch skin biopsy samples were obtained before and 48h after surgery from 35 participants (Figure 2) who underwent esophagectomy or liver resection (mean age:68y (9); 31% female; Supplementary data). No biopsy sites became infected. Patients who failed to achieve normal DO₂ were more likely to sustain serious complications (including sepsis) after surgery (Figure 3A), compared to 14/27 (51.8%) patients who achieved their individualised preoperative DO₂ target (absolute risk reduction:36% (95% confidence intervals:6 to 65%)).

Primary outcome: protein expression after surgery, stratified by oxygen delivery.

Label free proteomic analysis was undertaken in 17 patients who underwent esophagectomy (Table 1). We identified 2096 proteins in skin biopsy samples, of which 157 were differentially expressed ≥ 1.5 -fold after surgery independent of oxygen delivery ((median confidence score:124 (62-252); supplementary data). Fourteen out of 2096 detected proteins distinguished normal (n=10) versus low (n=7) DO₂ values after oesophagectomy (as illustrated by heatmap in Figure 3B).

Secondary outcomes: systems biology analysis.

To further dissect potential molecular interactions using Ingenuity Pathway Analysis (Figure 4A), we directly compared expression proteins before and after surgery for individuals who had either normal or low DO₂ after the trial intervention. In ten participants with normal DO₂, the expression of 65 proteins differed after surgery. In participants with low DO₂ values (n=7), 92 proteins changed after surgery (median confidence score:116 (62-223); supplementary data). Pathways involved in nervous system and renal injury were activated in patients with low DO₂ (Figure 4B). In skin, we found that proteins involved in leukocyte

activation and smooth muscle migration pathways (Figure 4C) pathways were upregulated in patients with normal DO₂. In particular, increased expression of the antimicrobial bactericidal peptidoglycan recognition protein-1 (PGLYRP-1) was observed.^{26 27} By contrast, in patients with low DO₂, proteins involved in epithelial necrosis with established roles in oxidative stress (superoxide dismutase-1, DJ-1/PARK7) and wound healing (CD44, thrombospondin, plasminogen, retinal binding protein-4) were differentially expressed compared to achievers (Figure 4C).

Immunohistochemical and immunoblot confirmation of proteomic findings.

To establish the generalisability of the proteomic data from skin biopsies obtained after oesophagectomy, separate external validation of specific proteins was also undertaken. We randomly selected skin biopsies from six individuals obtained before and after hepatic surgery for protein quantification by immunohistochemistry. We focused on proteins identified by mass spectrometry for which there were antibodies that have been validated for skin immunohistochemistry (Figure 5A). Expression levels of CD44 (the principal cell surface receptor for hyaluronate) and $\alpha 6\beta 4$ integrin (which stabilizes skin through the formation of hemidesmosomes) were reduced after surgery (Figure 5B). These changes were mirrored by semi-quantitative immunoblots and were also found in a murine model of hepatectomy (Supplementary data).

Discussion

We found that serial proteomic analysis of skin biopsies revealed a link between low oxygen delivery, oxidative stress and reparative processes previously identified by gene knockout experiments. The proteomic data from patients was verified by immunohistochemistry using selected antibodies that have been validated for immunohistochemistry in skin. Taken together, these data show that serial skin biopsies provide mechanistic insight into organ injury after surgery.

The complex composition in skin of proteins, metabolites and lipids, coupled with immunological surveillance and neural innervation, has led to the frequent use of skin biopsies to aid in the diagnosis of several hereditary neurologic metabolic disease.²⁸ Thus, insights into numerous genetic diseases have been afforded by skin biopsies, even though the disease doesn't primarily affect skin. However, despite the accessibility of skin, human proteomic studies are scarce.²⁹ In part, this reflects that skin has presented significant challenges for conventional proteomic techniques due to its high lipid content, insolubility and extensive cross-linking of proteins, all of which complicate the isolation and digestion of proteins for analysis using mass spectrometry techniques.¹⁷ This study was facilitated by recent advances in on-line fractionation and optimised acquisition protocols utilising ion mobility separation technology, which has increased the scope for protein identification more than ten-fold from a single punch biopsy.¹⁷ Our study extends previous proteomic analysis of plasma obtained from older adults undergoing elective surgery, which identified 564 proteins with altered expression levels altered after surgery.³ We demonstrate that tracking proteomic changes using skin biopsies is acceptable to surgical patients, easy to perform and provides integrated mechanistic insights into end-organ physiology that is seldom reflected by changes in circulating proteins in blood.

The proteomic profiles revealed by our study have captured components from each of

the four dynamic overlapping processes required for the coordination of successful healing of skin wounds.³⁰ Briefly, haemostasis is triggered once platelets encounter collagen and the extracellular matrix. The development of fibrin clot and release of clotting factors, growth factors and cytokines initiates the inflammatory phase, which lasts for ~48h (i.e. the timeframe over which the two skin punch biopsies were taken in our study). The inflammatory phase is heralded by the chemotaxis of neutrophils and monocyte/macrophages to commence phagocytosis of cellular debris and pathogens, assisted by the activation of mast cells and fibroblasts. New extracellular matrix is then created by deposition of collagen by fibroblasts and further remodelling facilitated by TGF β , proteoglycans, fibronectin and protease inhibitors.³¹ Our proteomic profiling ceased before the process of proliferation and epithelisation is widely held to be completed, which requires angiogenesis and neovascularisation.

Canonical pathway analysis highlighted that acute phase proteins and sirtuin signaling were markedly upregulated in patients with low oxygen delivery, suggesting that reduced oxygen delivery results in significant metabolic compromise. The sirtuins are a family of NAD⁺ dependent comprising class III histone deacetylases regulating the metabolic and transcriptomic response to oxidative stress in skin.²⁰ Activation of sirtuins 1-3 accelerate wound healing.³² At the individual protein level, we found a coordinated upregulation of antioxidant proteins including mitochondrial heat shock protein, deglycase DJ-1 and the mitochondrial antioxidant manganese superoxide dismutase. These changes were exclusively observed in patients where oxygen delivery was lower, suggesting strongly that failure to supply skin with adequate oxygen delivery during the early perioperative period results in delayed or persistent cellular metabolic stress for at least 36h after surgery. Our proteomic and immunohistochemical analysis also found decreased postoperative expression of CD44, the epidermal expression of which is required for optimal wound healing by maintaining

epidermal elasticity and resistance to stretch, as well as keratinocyte proliferation and differentiation.³³

Very few studies have focused on the molecular mechanisms underpinning the association between adequate perioperative oxygen delivery and reduced morbidity and/or mortality. Stroke volume guided fluid and low dose inotropic therapy was associated with improved oxygen delivery, microvascular flow and tissue oxygenation but had no impact on global (plasma) measures of inflammation after major surgery.³⁴ By contrast, proteomic analysis of skin biopsies obtained after surgery from patients with normal oxygen delivery after surgery demonstrated a coordinated leukocyte activation response that was absent in patients with low oxygen delivery. Moreover, normal oxygen delivery was associated with increased expression of the antimicrobial peptidoglycan recognition protein-1 (PGLYRP-1), which is expressed primarily in the granules of polymorphonuclear leucocytes and is present in neutrophil extracellular traps.²⁶ PGLYRP-1 is directly bactericidal for both Gram-positive and negative bacteria by interacting with cell wall peptidoglycan, rather than permeabilizing bacterial membranes.²⁷

The ubiquitin–proteasome system degrades intracellular proteins into peptide fragments that can be presented by major histocompatibility complex (MHC) class I molecules. Unique to low oxygen delivery group was the increased expression of PSMB9, one of two critical immunoproteasome subunits that degrade cell proteins to generate peptides for antigen presentation exclusively during acute inflammation.³⁵ Immunoproteasome expression is closely associated with T-cell infiltration, through cytokine production and T cell expansion and/or survival, by regulating apoptotic machinery and/or transcription factor activation.³⁶

We also noted that increased expression of thrombospondin-1 and plasminogen in both groups. The presence of thrombospondin-1 (TSP-1), a potent

chemotactic factor for monocytes and neutrophils, in skin biopsy samples 48h after surgery is consistent with its role in the early inflammatory phase of wounds; absence of TSP-1 delays wound healing.³⁷ However, given that we did not acquire further biopsy samples beyond 48h of surgery, we cannot exclude that the deleterious effects of persistently elevated expression of wound bed TSP1 prevents effective wound healing over the longer term.³⁸ The early presence of plasminogen in postoperative biopsy samples from both groups is also consistent with the critical role of this potent serine protease in triggering the resolution of inflammation and activating the proliferation phase of wound repair.³⁹ The observed increase in expression of kininogen, through which kinins are formed in the skin by the enzymatic action of tissue kallikrein, is consistent with its' role in skin homeostasis, wound healing and organ dysfunction more widely.⁴⁰

A strength of our study design was the within-subject comparison of punch biopsies within a similar abdominal area, thereby serving as a robust internal control. The masked analysis of samples to trial allocation is another strength. There are several limitations of this 'first-in-man' study of surgical patients. Samples obtained as part of a randomised controlled study in a specific subset of patients at higher risk of perioperative morbidity may not be generalizable across all surgical populations. By extension from murine experimental work, we surmised that low global oxygen delivery would result in lower skin oxygen delivery but this was not directly measured in skin. The proteins selected for immunohistochemical validation represent only a small subset of the proteins impacted by surgery and were chosen based on the availability of validated antibodies for immunohistochemistry, systems biology analysis, and literature supporting a link with skin-specific pathology. Due to cost and patient-related constraints, further samples beyond 48h after surgery were not obtained during the proliferative reparative phase. Usually, punch biopsies heal 5-10 days after the procedure, which would have lent itself to monitoring the

rate of healing if the patients had been guaranteed to reside in hospital until the punch biopsy site had healed. A derivation-validation approach correlated with postoperative outcomes would add further value.

In summary, serial skin biopsies identified novel surgery-specific protein changes in adults undergoing major elective noncardiac surgery. This approach may identify potential biomarkers with clinical utility, particularly as we observed upregulation of biomarkers over time. Proteomic analysis of skin biopsies provides further understanding of perioperative end-organ dysfunction, including the potential development of precision medicine-guided treatments for wound healing after major surgery.⁴¹

Acknowledgments

This work is supported by the UK NIHR Great Ormond Street Hospital Biomedical Research Centre. The views expressed are those of the author(s) and not necessarily those of the NHS, the NIHR or the UK Department of Health.

Author contributions

Study design: GLA

Study conduct: SI, LGP, AJT, AGDA, GLA, KM, WEH

Experiments: WEH, EB, FB, TJ, AGDA, KM, GLA

Data analysis: WEH, FB, MC, EAT, AGDA, GLA, KM

Drafting/revising manuscript: GLA, WEH, MC, TJ, AJT, AGDA, EAT, KM

Figure Legends

Figure 1. Methods and analysis.

- A. Schematic showing timing of serial skin biopsies before induction of anaesthesia and 48h after the haemodynamic trial intervention.
- B. Venn diagram showing primary and secondary outcome analyses. Blue shading/text denotes patients in whom oxygen delivery remained low after intervention. Red shading/text denotes patients in whom oxygen delivery was normal after intervention. Primary outcome was comparison between proteins differentially expressed in patients with normal versus low oxygen delivery after intervention. Grey shaded area highlights secondary pathway analyses which accounted for directional changes in protein expression for patients with normal or low DO₂ value. An increase/decrease was defined by fold-change >1.5, confidence score >20 and p value <0.05 (ANOVA), as generated by Progenesis QI analysis software.

Figure 2. Recruitment of participants into skin biopsy sub-study.

Asterisk denotes 3 paired samples that were used for proteomics and immunoblotting [biopsies were divided in half].

Figure 3. Proteomic differences in skin associated with perioperative oxygen delivery.

- A. Oxygen delivery expressed as percentage of preoperative oxygen delivery (measured before induction of anaesthesia). P values refers to comparison between subjects with normal versus low oxygen delivery over each hour during the 6h intervention period following surgery.

B. 14 proteins that were differentially expressed after surgery in non- DO₂ achievers and DO₂ achievers (median confidence score:63.7 (27.1-128.5)). Heatmap data is shown for relative changes for within-protein comparisons, for subjects with normal versus low oxygen delivery during trial intervention.

Figure 4. Postoperative differences in protein expression related to oxygen delivery intervention.

- A. Key for bioinformatic prediction of up/downregulated proteins and/or activation or inhibition of protein function.
- B. Canonical pathway analysis for enriched signaling categories in organ-specific injury pathways identified through differential proteins expression between in patients in whom oxygen delivery target was achieved versus non-achievers.
- C. Canonical pathway analysis for enriched signaling categories in skin-specific pathways for patients who achieved, or failed to achieve their individualized preoperative DO₂ value.

Figure 5. Immunohistochemistry validation of selected proteins.

- A. TRITC (tetramethylrhodamine) fluorescence for CD44 and ITGA6 was compared before and 48h after surgery in skin samples added to 10% formalin immediately after punch biopsy was performed. DAPI (4',6-diamidino-2-phenylindole) staining identifies cell nuclei. Scale bar:100µm
- B. Summary data for epidermal fluorescence for CD44 and ITGA6 proteins, compared before and after surgery (standardised to group mean fluorescence levels before surgery; n=6 patients).

References

- 1 Zhang B, Whiteaker JR, Hoofnagle AN, Baird GS, Rodland KD, Paulovich AG. Clinical potential of mass spectrometry-based proteogenomics. *Nat Rev Clin Oncol* 2019; **16**: 256-68
- 2 Bantscheff M, Lemeer S, Savitski MM, Kuster B. Quantitative mass spectrometry in proteomics: critical review update from 2007 to the present. *Anal Bioanal Chem* 2012; **404**: 939-65
- 3 Fong TG, Chan NY, Dillon ST, et al. Identification of Plasma Proteome Signatures Associated With Surgery Using SOMAscan. *Ann Surg* 2019
- 4 Mukai A, Suehiro K, Watanabe R, et al. Impact of intraoperative goal-directed fluid therapy on major morbidity and mortality after transthoracic oesophagectomy: a multicentre, randomised controlled trial. *Br J Anaesth* 2020; **125**: 953-61
- 5 Khuri SF, Henderson WG, DePalma RG, Mosca C, Healey NA, Kumbhani DJ. Determinants of long-term survival after major surgery and the adverse effect of postoperative complications. *Ann Surg* 2005; **242**: 326-41
- 6 Wu WC, Smith TS, Henderson WG, et al. Operative blood loss, blood transfusion, and 30-day mortality in older patients after major noncardiac surgery. *Ann Surg* 2010; **252**: 11-7
- 7 Pearse RM, Harrison DA, MacDonald N, et al. Effect of a perioperative, cardiac output-guided hemodynamic therapy algorithm on outcomes following major gastrointestinal surgery: a randomized clinical trial and systematic review. *JAMA* 2014; **311**: 2181-90
- 8 Ackland GL, Iqbal S, Paredes LG, et al. Individualised oxygen delivery targeted haemodynamic therapy in high-risk surgical patients: a multicentre, randomised, double-blind, controlled, mechanistic trial. *Lancet Respir Med* 2015; **3**: 33-41
- 9 Peerless JR, Alexander JJ, Pinchak AC, Piotrowski JJ, Malangoni MA. Oxygen delivery is an important predictor of outcome in patients with ruptured abdominal aortic aneurysms. *Ann Surg* 1998; **227**: 726-32; discussion 32-4
- 10 Hotamisligil GS. Inflammation, metaflammation and immunometabolic disorders. *Nature* 2017; **542**: 177-85
- 11 Jonsson K, Jensen JA, Goodson WH, 3rd, et al. Tissue oxygenation, anemia, and perfusion in relation to wound healing in surgical patients. *Ann Surg* 1991; **214**: 605-13
- 12 Catania RA, Schwacha MG, Cioffi WG, Bland KI, Chaudry IH. Does uninjured skin release proinflammatory cytokines following trauma and hemorrhage? *Arch Surg* 1999; **134**: 368-73; discussion 73-4
- 13 Bos JD. The skin as an organ of immunity. *Clin Exp Immunol* 1997; **107 Suppl 1**: 3-5
- 14 Kabashima K, Honda T, Ginhoux F, Egawa G. The immunological anatomy of the skin. *Nat Rev Immunol* 2019; **19**: 19-30
- 15 Hope JC, Dearman RJ, Kimber I, Hopkins SJ. The kinetics of cytokine production by draining lymph node cells following primary exposure of mice to chemical allergens. *Immunology* 1994; **83**: 250-5
- 16 Clavien PA, Strasberg SM. Severity grading of surgical complications. *Ann Surg* 2009; **250**: 197-8
- 17 Bliss E, Heywood WE, Benatti M, Sebire NJ, Mills K. An optimised method for the proteomic profiling of full thickness human skin. *Biol Proced Online* 2016; **18**: 15
- 18 Distler U, Kuharev J, Navarro P, Levin Y, Schild H, Tenzer S. Drift time-specific collision energies enable deep-coverage data-independent acquisition proteomics. *Nat Methods* 2014; **11**: 167-70
- 19 Geromanos SJ, Vissers JP, Silva JC, et al. The detection, correlation, and comparison of peptide precursor and product ions from data independent LC-MS with data dependant LC-MS/MS. *Proteomics* 2009; **9**: 1683-95
- 20 Perez-Riverol Y, Csordas A, Bai J, et al. The PRIDE database and related tools and resources in 2019: improving support for quantification data. *Nucleic Acids Res* 2019; **47**: D442-D50
- 21 Szklarczyk D, Gable AL, Lyon D, et al. STRING v11: protein-protein association networks with increased coverage, supporting functional discovery in genome-wide experimental datasets. *Nucleic Acids Res* 2019; **47**: D607-D13

- 22 The Gene Ontology C. The Gene Ontology Resource: 20 years and still GOing strong. *Nucleic Acids Res* 2019; **47**: D330-D8
- 23 Kanehisa M, Sato Y, Furumichi M, Morishima K, Tanabe M. New approach for understanding genome variations in KEGG. *Nucleic Acids Res* 2019; **47**: D590-D5
- 24 Huang da W, Sherman BT, Lempicki RA. Systematic and integrative analysis of large gene lists using DAVID bioinformatics resources. *Nat Protoc* 2009; **4**: 44-57
- 25 Kramer A, Green J, Pollard J, Jr., Tugendreich S. Causal analysis approaches in Ingenuity Pathway Analysis. *Bioinformatics* 2014; **30**: 523-30
- 26 Cho JH, Fraser IP, Fukase K, et al. Human peptidoglycan recognition protein S is an effector of neutrophil-mediated innate immunity. *Blood* 2005; **106**: 2551-8
- 27 Dziarski R, Kashyap DR, Gupta D. Mammalian peptidoglycan recognition proteins kill bacteria by activating two-component systems and modulate microbiome and inflammation. *Microb Drug Resist* 2012; **18**: 280-5
- 28 Carpenter S. Skin biopsy for diagnosis of hereditary neurologic metabolic disease. *Arch Dermatol* 1987; **123**: 1618-21
- 29 de Veer SJ, Furio L, Harris JM, Hovnanian A. Proteases and proteomics: cutting to the core of human skin pathologies. *Proteomics Clin Appl* 2014; **8**: 389-402
- 30 Gurtner GC, Werner S, Barrandon Y, Longaker MT. Wound repair and regeneration. *Nature* 2008; **453**: 314-21
- 31 Werner S, Grose R. Regulation of wound healing by growth factors and cytokines. *Physiol Rev* 2003; **83**: 835-70
- 32 Spallotta F, Cencioni C, Straino S, et al. A nitric oxide-dependent cross-talk between class I and III histone deacetylases accelerates skin repair. *J Biol Chem* 2013; **288**: 11004-12
- 33 Shatirishvili M, Burk AS, Franz CM, et al. Epidermal-specific deletion of CD44 reveals a function in keratinocytes in response to mechanical stress. *Cell Death Dis* 2016; **7**: e2461
- 34 Jhanji S, Vivian-Smith A, Lucena-Amaro S, Watson D, Hinds CJ, Pearse RM. Haemodynamic optimisation improves tissue microvascular flow and oxygenation after major surgery: a randomised controlled trial. *Critical Care* 2010; **14**: R151
- 35 Kruger E, Kloetzel PM. Immunoproteasomes at the interface of innate and adaptive immune responses: two faces of one enzyme. *Curr Opin Immunol* 2012; **24**: 77-83
- 36 Thomas C, Tampe R. MHC I chaperone complexes shaping immunity. *Curr Opin Immunol* 2019; **58**: 9-15
- 37 Agah A, Kyriakides TR, Lawler J, Bornstein P. The lack of thrombospondin-1 (TSP1) dictates the course of wound healing in double-TSP1/TSP2-null mice. *Am J Pathol* 2002; **161**: 831-9
- 38 Isenberg JS, Pappan LK, Romeo MJ, et al. Blockade of thrombospondin-1-CD47 interactions prevents necrosis of full thickness skin grafts. *Ann Surg* 2008; **247**: 180-90
- 39 Sulniute R, Shen Y, Guo YZ, et al. Plasminogen is a critical regulator of cutaneous wound healing. *Thromb Haemost* 2016; **115**: 1001-9
- 40 Chao J, Shen B, Gao L, Xia CF, Bledsoe G, Chao L. Tissue kallikrein in cardiovascular, cerebrovascular and renal diseases and skin wound healing. *Biol Chem* 2010; **391**: 345-55
- 41 Lisboa FA, Dente CJ, Schobel SA, et al. Utilizing Precision Medicine to Estimate Timing for Surgical Closure of Traumatic Extremity Wounds. *Ann Surg* 2019; **270**: 535-43

Table 1: Subject characteristics.

Data shown for participants who underwent goal-directed therapy after oesophagectomy or hepatobiliary surgery aimed at achieving their preoperative oxygen delivery and had paired skin biopsies taken. Data are presented as mean (standard deviations; SD) for parametric data and as median (25th-75th interquartile range) for non-parametric data. Frequencies are presented with percentages (%). Age is rounded to the nearest year. *indicates sepsis or suspected infection within 72h of surgery. ¹- inhalational general anaesthesia was used in all cases.

	Skin biopsies (oesophagectomy)		All participants	
	Normal Do ₂ (n=10)	Low Do ₂ (n=7)	Normal Do ₂ (n=22)	Low Do ₂ (n=9)
Age (y)	67 (6)	67 (4)	71 (10)	69 (4)
Female sex (n;%)	4 (31%)	3 (43%)	10 (45%)	4 (44%)
Body mass index (kg m ⁻²)	28.5 (4.0)	28.4 (2.8)	27.7 (4.1)	28.3 (4.0)
Haemoglobin (g l ⁻¹)	121 (15)	139 (20)	125 (15)	135 (23)
Albumin (g l ⁻¹)	42 (5)	45 (2)	44 (5)	44 (3)
Co-morbidities (n; %)				
Cardiovascular disease	12 (71%)	4 (57%)	19 (86%)	7 (78%)
Diabetes mellitus	3 (18%)	0	5 (23%)	1 (11%)
Hypertension	8 (47%)	3 (43%)	14 (64%)	5 (56%)
Intraoperative				
General ¹ + epidural anaesthesia	11 (65%)	7 (100%)	17 (77%)	8 (89%)
Duration of operation (mins)	260 (195-335)	298 (288-360)	273 (102)	319 (83)
Fluid therapy (ml.kg.h)	7.1 (4.8-11.7)	8.8 (7.3-10.6)	9.6 (6.3-14.5)	11.3 (4.1)
Packed red cells (n;%)	3 (18%)	1 (14%)	1	1
Lactate (mmol l ⁻¹)	2.4 (1.2-3.0)	1.8 (1.7-2.4)	1.7 (1.2-2.6)	2.1 (1.7-2.4)
Intervention period				
Dobutamine	3 (30%)	1 (14%)	5 (23%)	1 (11%)
Fluid therapy (ml.kg.h)	20.5 (16.5-25.0)	16.9 (12.9-23.0)	18.4 (13.1-24.7)	21.2 (15.4-24.8)
Packed red cells (n;%)	2 (22%)	0	2 (9%)	3 (33%)
Lactate (mmol l ⁻¹)	2.4 (1.2-3.0)	1.8 (1.7-2.4)	1.9 (0.9-2.6)	1.3 (1.2-2.5)
Haemoglobin (g l ⁻¹)	114 (18)	122 (18)	113 (16)	114 (22)
Complications				
Clavien-Dindo > grade 2 (n;%)	5 (50%)	5 (74%)	11 (50%)	6 (67%)
Infection/sepsis* (n;%)	5 (50%)	4 (57%)	7 (32%)	5 (56%)
Length of hospital stay (days)	16 (10-27)	24 (17-78)	12 (8-17)	17 (12-22)

Figure 1

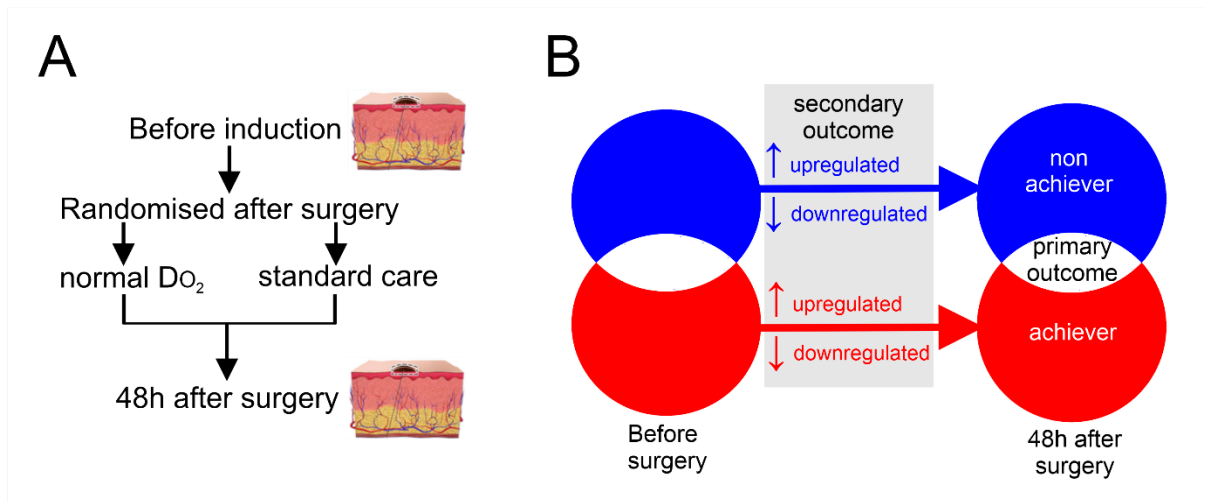


Figure 2

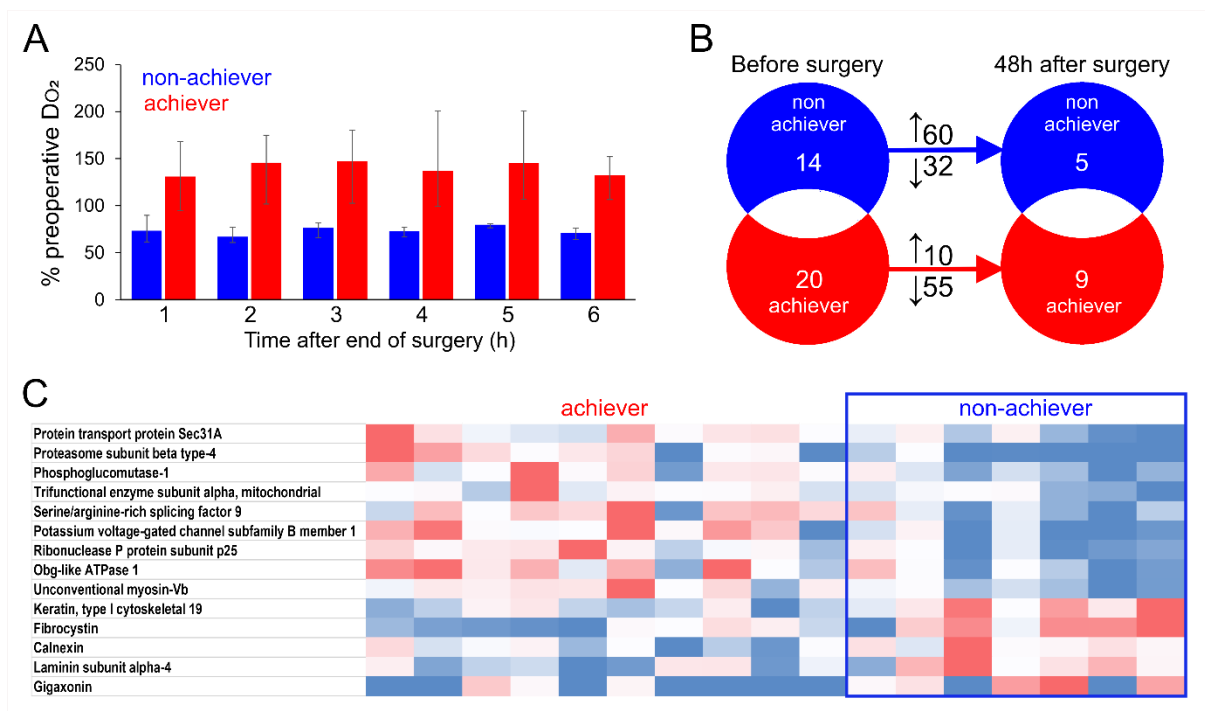


Figure 3

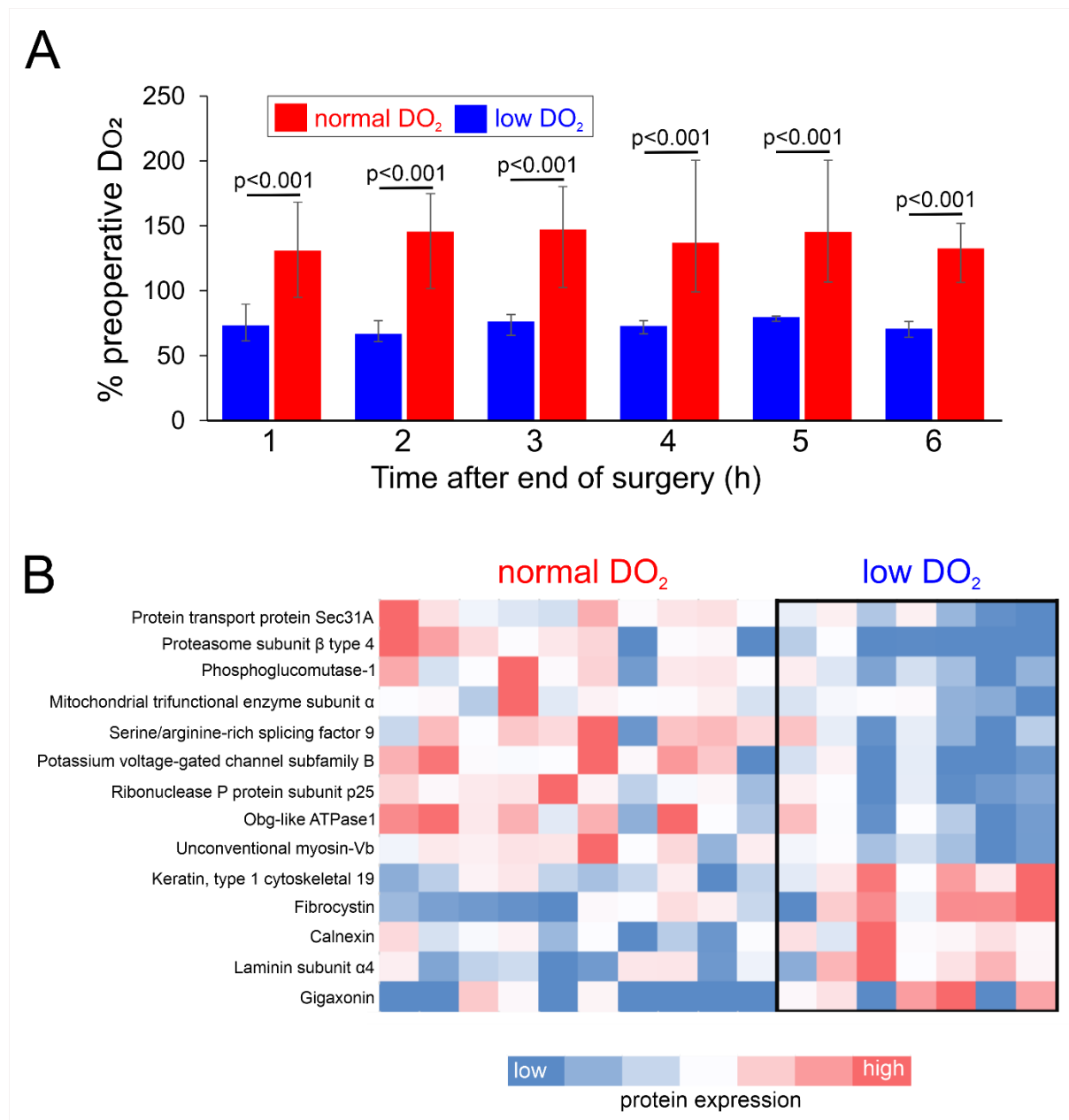
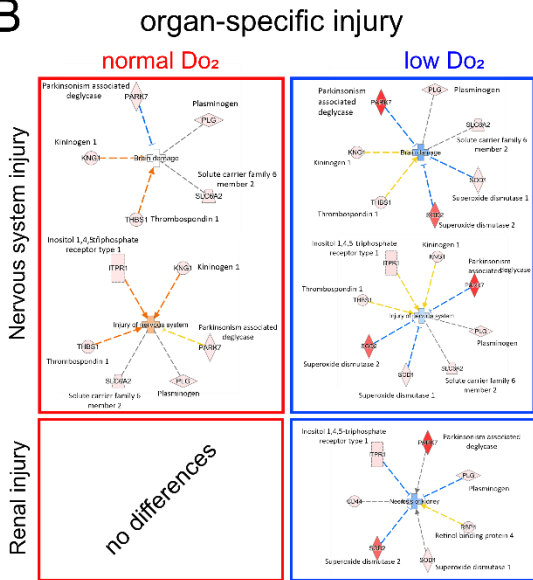


Figure 4

A



B



C

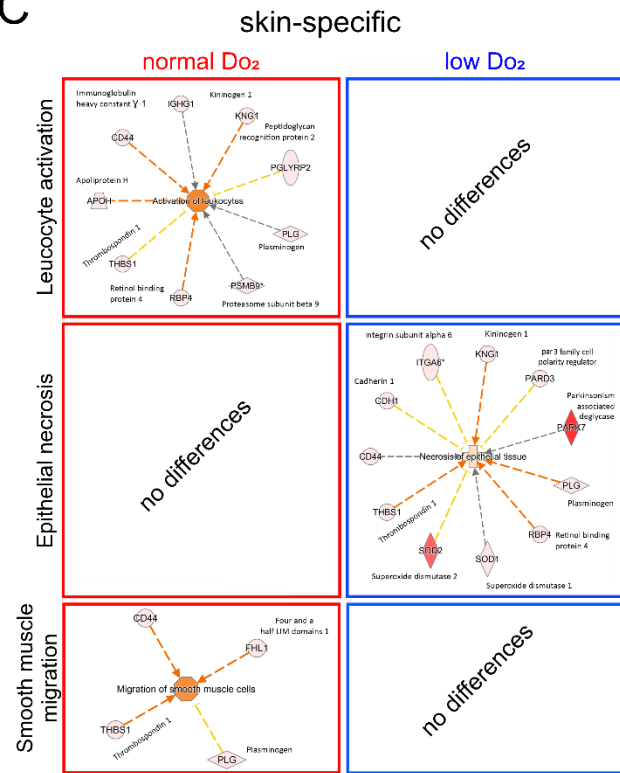


Figure 5

